Development of Next-Generation PFDHA Using High-resolution Geodetic Imaging Data

Report for SCEC Award #19222

Investigators: Andrea Donnellan, Chris Milliner (Co-PI), Rui Chen (Co-PI)

I. Project Overview

A. Abstract

Describe the project objectives, methodology, and results obtained and their significance. If this work is a continuation of a multi-year SCEC-funded project, please include major research findings for all previous years in the abstract. (Maximum 250 words.)

PFDHA is a probabilistic approach to characterize the hazard of distributed rupture that is used by engineers and hazard practitioners to safely design distributed infrastructure (e.g., gas and water pipelines, roads and bridges) that cannot avoid fault crossings. The primary limitation with the current PFDHA approach is that the probability models are constrained solely by field observations which are spatially sparse and have unknown uncertainties, which limit the model's predictive power. Here our primary aim was to use pixel tracking techniques applied to satellite optical images to measure the magnitude, width and distribution of coseismic inelastic strain from recent surface ruptures to better constrain the probability of distributed fault rupture. Results from this project include, processing of satellite data to produce displacement maps of 9 earthquakes, modifying the PFDHA theory to incorporate the geodetic data, and generating geodetic-based fault displacement prediction equations to calculate fault displacement hazard maps. In addition, part of this work has led to an SRL publication (Milliner & Donnellan, 2020), helping understand the fracture distribution and timing during the M_w 7.1 2019 Ridgecrest earthquake sequence. Results derived from this project have been invaluable as they have helped secure a larger scale 3-year project funded by a NASA ROSES-ESI grant, to further advance the geodetic-based PFDHA approach. These next-generation geodetic-based PFDHA models will provide engineers with higher confidence on the likelihood of distributed rupture, and the data gathered here will help in validation of dynamic elastoplastic rupture simulations which could set the foundations towards a non-ergodic PFHDA approach.

B. SCEC Annual Science Highlights

Each year, the *SCEC Science Planning Committee* reviews and summarizes SCEC research accomplishments, and presents the results to the SCEC community and funding agencies. Rank (in order of preference) the sections in which you would like your project results to appear. Choose up to 3 working groups from below and order them according to your preference ranking. The list is pre-populated with the SCEC groups you selected during proposal submission.

i) Tectonic Geodesy
ii) Earthquake Engineering Implementation Interface (EEII)
iii) Earthquake Geology

C. Exemplary Figure

Select one figure from your project report that best exemplifies the significance of the results. The figure may be used in the SCEC Annual Science Highlights and chosen for the cover of the

Annual Meeting Proceedings Volume. In the box below, enter the figure number from the project report, figure caption and figure credits.

Figure 4

D. SCEC Science Priorities

How does the project contribute to the overall intellectual merit of SCEC? For example: *How does the research contribute to advancing knowledge and understanding in the field and, more specifically, SCEC research objectives? To what extent has the activity developed creative and original concepts?*

P1.a, **P3.d** and **P3.e**

E. Intellectual Merit

How does the project contribute to the overall intellectual merit of SCEC? *For example: How does the research contribute to advancing knowledge and understanding in the field and, more specifically, SCEC research objectives? To what extent has the activity developed creative and original concepts?*

The project addresses:

- What is the spatial distribution of inelastic strain? So far, most studies have provided scalar estimates of the amount of coseismic off-fault inelastic deformation. The across-fault spatial distribution has been captured in long-term geologic and geomorphic studies of faults and in specific instances along surface ruptures from offset man-made markers. Here we have attempted to define what functional form characterizes the spatial attenuation of inelastic strain with distance away from the rupture, which also allows us to create fault displacement prediction equations for PFDHA.
- What factors control off-fault deformation and distributed inelastic strain? What is the effect of fault compression and extension that is difficult to measure in the field? Here we used geodetic observations of the Ridgecrest earthquake rupture and created 2D strain maps to assess how the fault zone width and distribution of inelastic strain varied with varying amounts of fault zone compression and extension.
- Improving the PFDHA method which so far is constrained only by field-based data. We have developed an independent but complementary approach that uses high-resolution geodetic imaging data that can measure the spatial distribution of displacement across surface ruptures. Here we have developed new probabilistic theory and hazard equations.
- This project has also helped established new collaborations within SCEC including engineers at UCLA (Prof. Yousef Bozorgnia) who are developing a database of past earthquake ruptures, and hazard practitioners at consultancy firms at PG&E, LCI, and various state agencies (including Caltrans and CGS).

F. Broader Impacts

How does the project contribute to the broader impacts of SCEC as a whole? For example: *How well has the activity promoted or supported teaching, training, and learning at your institution or across SCEC? If your project included a SCEC intern, what was his/her contribution? How has your project broadened the participation of underrepresented groups? To what extent has the project enhanced the infrastructure for research and education (e.g., facilities, instrumentation, networks, and partnerships)? What are some possible benefits of the activity to society?)*

- This project has led to training and professional development of a postdoc (C.M.).
- The research has led to increased collaboration between researchers at JPL and hazard practitioners at California Geological Survey at Sacramento and San Mateo.
- This work has important societal benefits as it will help create a better-informed design criteria for engineers to build more resilient infrastructure ultimately helping protect critical lifelines such as, road, bridges, and water, gas and telecommunicates pipelines that are vulnerable to damage at fault crossings e.g., Elizeabth Lake near Palmdale and the I-5 at Cajon pass.

G. Project Publications

All publications and presentations of the work funded must be entered in the SCEC Publications database. Log in at *http://www.scec.org/user/login* and select the Publications button to enter the SCEC Publications System. Please either (a) update a publication record you previously submitted or (b) add new publication record(s) as needed. If you have any problems, please email *web@scec.org* for assistance.

II. Technical Report

A. Introduction & Rationale

Distributed inelastic strain, also termed off-fault deformation (OFD), is known to affect the propagation of the rupture, radiation of seismic energy, accumulation of elastic strain, and poses a significant hazard to the urban environment (Dunham et al., 2011; Roten et al., 2017). However, it also poses a significant hazard to buildings already situated next to newly discovered faults, and distributive infrastructure such as pipelines, bridges, communication lines, or railroads, which cannot avoid fault crossing. Probabilistic fault displacement hazard analysis (PFDHA), is a probabilistic approach to quantify the annual rate of exceeding some distributed strain. The hazard curves are estimated using "fault displacement prediction equations" (FDPEs) that characterize the amplitude and distribution of co-seismic fault displacement on and off the primary rupture. FDPEs are developed empirically using fault displacement data following an ergodic approach, where the means and standard deviations of distributed displacement are used to calculate the conditional probabilities of exceedance in hazard integrations. So far PFDHA models have been constrained solely by traditional field measurements and mapping of the co-seismic surface rupture (Chen and Petersen, 2011; Petersen et al., 2011). Although these point-measurements are valuable in-situ observations of displacement, they are also sparsely populated in the near-field region due to a lack of cultural offset markers that span the entire fault zone and are subject to large uncertainty that is difficult to define (Rockwell et al., 2002; Scharer et al., 2014). In turn, this results in probability models that have large uncertainties and limited predictive power.

Objectives

Here we propose to develop a new approach to PFHDA by using measurements of distributed co-seismic strain from high-resolution surface deformation maps of recent large magnitude (M_w>6.0) earthquakes using subpixel image correlation. Specific objectives of this project include:

1. Acquire high-resolution satellite imagery of 11 earthquakes to measure width, magnitude and distribution of total displacement across the surface rupture.
2. Develop automated and objective tools to extract fault displacement from image correlation maps, so to create a reproducible dataset and improve upon the current approach which is manual and subjective that may introduce epistemic uncertainty.
3. Modify the probability theory (i.e., the hazard equations) of the current PFDHA to incorporate geodetic data (which measures shifts of patches of an image), as currently it is developed for field data (which measures discrete offsets at a point).
4. Compile geodetic displacement data from multiple surface ruptures to develop regressions of fault displacement that characterize i) along-strike variation of total displacement and ii) across-strike variation (i.e., 'fall-off') of secondary displacement and inelastic strain.
5. Create fault displacement hazard maps that detail the amount of displacement given a certain probability and exposure time (typically 10% over 50-year exposure time).
6. Develop and foster a multidisciplinary collaboration network composed of researchers, hazard practitioners and engineers who implement the hazard models to understand what they require.

B. Method overview

Here we summarize the full workflow we have developed from the correlation displacement maps (e.g., Fig. 1) to the fault displacement hazard maps (Fig. 4). In the next section we describe in detail the tools developed that were required to complete this workflow. First, to measure the surface displacement from an earthquake the optical images are orthorectified to correct for topographic and camera distortions using COSI-Corr. They are then correlated either with COSI-Corr's phase correlator or OR-Corr, a robust statistical image correlation algorithm that we have developed. Next, the location of the primary fault trace is determined using our automated least cost path analysis algorithm profiles. Then the fault parallel displacement (Fig. 1) are measured across the surface rupture from the displacement maps (Fig. 1a) using our template-based stacking method and automatic profile tool. Once the displacement profiles are collected for all the earthquakes, they are compiled and used to constrain the conditional probability of rupture occurrence by first calculating the gradient (transforming the profiles from fault parallel displacement to fault parallel shear strain) and then calculating the frequency of profiles that exceed an inelastic strain value (0.5% following Brooks et al., 2017, although we note this value is largely arbitrary). This provides an empirical probability as a function of distance that a site will experience inelastic strain (i.e., rock failure). As we have developed two distinct PFDHA models that characterize i) the probability of experiencing a certain amount of the total displacement (which includes both on and off-fault displacement which the optical correlation approach cannot distinguish) over a certain distance and ii) the likelihood of experiencing a certain amount of inelastic strain at a given point, where each requires a different means to constrain the conditional probability of exceedance. For the first hazard model the conditional probability of exceeding a certain amount of displacement requires specifying a distance over which the hazard should be calculated (i.e., the building footprint), which is constrained from the displacement profiles. While the conditional probability of exceeding a certain strain value at a point location is constrained from the shear strain profiles. For both cases the probability of exceedance is calculated from fault displacement (or strain) prediction equations (FDPE) which are constrained by fitting a functional form to how the displacement (or strain) decreases with distance away from the primary fault (e.g., Fig. 3b). From this fit the mean and standard deviation are used as the distribution parameters for a lognormal distribution, from which the survivor function is calculated and the conditional probability can then be estimated. Although we note, future work will address whether Weibull or Gamma distributions are more appropriate (e.g., Youngs et al., 2003). As the total displacement is normalized along the rupture length, this requires convolving the normalized total displacement exceedance probability with the probability of total displacement at the given location along the rupture, where the latter requires regressions for how displacement varies along a surface rupture. The along-fault displacement regressions are defined by first compiling and normalizing the total displacement as a function of normalized along-fault distance and folded at the rupture midpoint as we assume that any asymmetry of the slip profile cannot be predicted and becomes part of the epistemic uncertainty (although future work could address this assumption). Once the conditional probability of exceedance and occurrence have been constrained, the only other terms in the hazard equation (eq. 1 and 2) are the temporal recurrence (α) for a given range of earthquake magnitudes (second term in eq. 1 and 2), which are not addressed by our analysis and is constrained by paleoseismic or geodetic slip rates, seismic catalogues and/or earthquake rupture forecast simulations (e.g., UCERF).

C. Results

Below we have divided our results into methodological advancements and scientific results.

1. Methodological developments

Part of our work has involved developing a more robust statistical correlator which uses the Spearman rank to estimate the correlation score between images. This approach is more resistant to outliers than regular statistical correlators as the values of the outliers are limited to their rank value, and as such we have named

our correlation algorithm Outlier-Resistant Correlator (OR-Corr). Outliers may arise between the images due to changes from vegetation, building damage, or urban development, and we have found our approach produces more stable results in such regions. This new image correlator we have developed has been outlined in our recent publication of (Milliner and Donnellan, 2020), and is a complementary method to correlating images to COSI-Corr.

To measure the fault-parallel displacement and finite inelastic shear strain across the surface rupture requires projecting the north-south and east-west displacement maps into the fault parallel direction and then stacking the profiles in the along-strike direction to minimize noise. However, within the width of the stack swath (typically 100-200 m in the along-strike direction), standard stacking approaches assume a uniform fault orientation. This is problematic for our analysis as neglecting variations of the fault orientation when stacking causes averaging of different sides of the fault which soothes and artificially widens the true fault width and lowers the inelastic finite shear strains (e.g., red line in Fig. 2b). To correct for this we have developed a template based sub-pixel cross correlation algorithm that aligns each 'sub-profile' prior to stacking. We have found that the template-based stacking method vastly improves the result, by preserving the true width, distribution and gradients of displacement across the rupture (blue line Fig. 2b).

Part of the hazard models requires constraining how the displacement varies along the length of the rupture. Various models have been proposed to describe the coseismic slip distribution from triangular, sinusoid, elliptical and bi-linear (Manighetti et al., 2005). To measure the total displacement from each profile requires estimating the total amplitude of the offset from each profile. The current approach is largely subjective, requiring manual interpretation of how to fit linear segments to either side of the displacement discontinuity. Here we have developed an automated and objective total displacement estimation tool which fits a linear and error function to the data using a nonlinear regression approach (as the parameters are nonlinear in the model). This provides an approach to estimate the total displacement from all 9 earthquakes in a consistent and reproducible manner, which is vital if new displacement measurements are to be later added to further constrain the fault displacement probability models. Furthermore, this automated approach also helps reduce introducing additional variation into the dataset through epistemic uncertainty associated with how to manually interpret the displacement profiles.

Determining where the primary fault is located along a rupture is important for constraining the fault displacement prediction equations as it determines the co-ordinate system and location of the zero distance from which to model how displacement attenuates with distance away from the 'primary' fault. However, distinguishing between a primary vs. a secondary fault is a non-trivial problem and so far, the selection has relied upon experience or expert consensus. To provide an objective and automated approach we have used the least cost path algorithm which determines the path that minimizes both the distance and cost (using a certain cost function) from one pre-determined point to another (i.e., the two rupture end points, whose locations are the only subjective part of the workflow). For the cost function we chosen to minimize the inverse of the curl of the coseismic displacement vector field (which approximates the degree of fault shear as intensity of spin), with an exponential weighting. This means the fault trace algorithm attempts to minimize the distance between two rupture end points and follow locations that exhibit the highest amount of shear strain, forcing the primary rupture trace to follow faults that likely experienced the largest amounts of displacement. This automated approach now allows us to estimate the fault trace in a consistent and reproducible for different surface ruptures.

We have gathered geodetic data and processed correlation maps for four out of the five earthquake we originally proposed and included an additional event, the 2014 M_w 6.2 Nagano earthquake in Japan. The 2016 M_w 6.2 Amatrice was the only event we did not collect data for, but this is a normal faulting event and future work will address the rupture hazard of dip-slip faulting events. Although we gathered

data for four additional events, bringing the total number of earthquakes to 11, we found that the quality and resolution of the displacement results were either too poor or coarse for the 2011 M_w 6.2 Christchurch and 2018 M_w 7.5 Palu earthquakes. However, use of World View data for the Palu earthquake may provide a potential avenue for improved results. Overall, we feel the current dataset we have gathered is sufficient to constrain fault displacement hazard equations.

We note that once all of the displacement profiles have been extracted from the displacement maps of the 9 viable earthquakes (which will 3000-5000 profiles), they will be added to the fault displacement database being developed by the Fault Displacement Hazard Initiative group at UCLA led by Prof. Yousef Bozorgnia (*https://www.risksciences.ucla.edu/nhr3/fdhi/home*). This database will serve as the central data hub for PFDHA hazard modelers, similar to how the NGA database of seismic recordings is used to constrain ground motion attenuation equations for PSHA.

2. Project Results

As the optical image correlation measures displacement over an area and is therefore length scale dependent, while the field measurements are point-based and able to resolve discontinuities, we have developed two types of probability models (detailed by the two hazard equations, eq. 1 and 2) that are distinct but complementary to the current field-based PFDHA approach. The first hazard model estimates how the amount of total displacement (both principal and secondary, off-fault) varies across the fault-zone over a certain distance (i.e., building footprint size) because the optical approach of matching shifts of patches of images cannot distinguish between the primary, secondary and other off-fault deformation mechanisms (e.g., folding, grain boundary sliding, or smaller scale fracturing). The other hazard model we produce is the magnitude of inelastic shear strain at a point location (i.e., the gradient of the total displacement profiles). Unfortunately, this will make direct comparison and validation between field and geodetic-based probabilistic models and FDPE challenging, but future work aims to address this problem.

$$\lambda(Dd \geq Dd_o)_{xyz} = \alpha(m_0) \int_{m_{1,S}}^{m_{2,S}} f_{M,S}(m,s)\, \boldsymbol{P}[\boldsymbol{sr \neq 0 | m}] \cdot P(\varepsilon > \varepsilon_{inelastic} | z, r, sr \neq 0)\, \boldsymbol{P}(\boldsymbol{Dd \geq Dd_o} | \boldsymbol{r}, \boldsymbol{z}, \tfrac{\boldsymbol{l}}{\boldsymbol{L}}, \boldsymbol{m})\, dr\, dm\, ds \quad (1)$$

$$\lambda(\varepsilon \geq \varepsilon_o)_{xyz} = \alpha(m_0) \int_{m_{1,S}}^{m_{2,S}} f_{M,S}(m,s)\, \boldsymbol{P}[\boldsymbol{sr \neq 0 | m}] \cdot P(\varepsilon > \varepsilon_{inelastic} | z, r, sr \neq 0)\, \boldsymbol{P}(\boldsymbol{\varepsilon \geq \varepsilon_o} | \boldsymbol{r}, \tfrac{\boldsymbol{l}}{\boldsymbol{L}}, \boldsymbol{m})\, dm\, ds \quad (2)$$

Through a thorough statistical analysis of profiles collected from the Landers, Ridgecrest and Hector Mine earthquakes we have determined the appropriate functional form that best describes the attenuation of displacement with distance from the fault is an error function. Although we cannot reject the hypothesis that an arctan or exponential function provides a statistically better fit, the error function provides the overall lowest misfit and we use this function to define the FDPE. We have also compiled along-strike displacement distributions from all of the 9 earthquakes which has provided new geodetic-based displacement-length scaling relations (Fig. 3a) that will be fundamental to calculating the hazard in PFDHA and will likely have use for those in the earthquake geology and paleoseismologic communities.

In this project we measured the surface displacement of the Ridgecrest earthquake using PlanetLabs satellite imagery to help decipher the timing of fracturing and separate surface deformation between the foreshock and mainshock. Unfortunately, we found the Planet Labs imagery (which was free data) had insufficient resolution and noise that was too large for our purpose of measuring inelastic strain across the rupture. However, SPOT-5 imagery (1.5 m resolution) was purchased using funds from this project, has produced very useful measurements of the near-field strain (fig. 1), and our analysis of this dataset is in the final stages of another paper submission that C.M. is leading. One of the main results from this dataset is

that we found measurements of inelastic strain of the Ridgecrest earthquake reveals a clear dependence on the degree of fault zone compression and extension. Such a result we believe will be of interest to the earthquake geology and fault mechanics communities and will be considered as a key factor to now include in the PFDHA approach as it affects the width of rupture and therefore the hazard (Fig. 2a).

From our FDPE constrained using an error function fit to the variation of displacement across the Landers rupture (Fig. 3b) and variation along the rupture (Fig. 3a) we have created preliminary fault displacement hazard maps using eq. 1 (see Fig. 4). Going forward the inclusion of displacement profiles from the other 7 earthquakes and consideration of their uncertainties and covariances using a mixed effects model will help provide more accurate estimates of the hazard. We also plan to include the effect of fault zone dilation and compression, different types of materials and sediment thickness, which will be explored in future work. The results described in this report (Figs. 1-4) were presented at an oral session at AGU and poster at SCEC and were planned for another oral session at SSA, but was subsequently canceled.

Over the longer-term we plan to produce fault displacement hazard maps that will be calculated by connecting our fault displacement prediction equations (FDPE) to UCERF, much like how seismic shaking hazard maps are estimated using UCERF with empirical ground motion prediction equations (GMPE). In addition, it is also important that we work towards a non-ergodic PFDHA approach. Over the long-term this will likely be achieved by sharing the geodetic fault displacement profiles and FDPE with the dynamic rupture modeling community to validate and constrain their physics based numerical rupture simulations of dynamic plastic yielding at the surface (e.g., Ma and Andrews, 2010; Roten et al., 2017). This is essentially equivalent to the direction PSHA is now taking, which is moving away from using empirical GMPE and towards physics-based simulations of seismic shaking (e.g., with CyberShake Graves et al., 2011).

D. Conclusions

Our project has been the first attempt to incorporate geodetic data into the PFDHA approach, which currently relies solely upon field observations. The optical image correlation technique provides an opportunity to improve the PFDHA method by using measurements of fault displacement and inelastic strain across the entire width of the surface rupture, which have high spatially density and uncertainty that can be quantified. Due to the geodetic imaging data being different in nature to the field observations, we have developed two characterizations of PFDHA models. The first estimates how the total displacement (both principal and secondary, off-fault) varies across the rupture over a given distance (e.g., the building footprint size) and the second the magnitude of inelastic shear strain at a point location.

Our project has generated displacement maps for 9 earthquakes (e.g., Fig. 1), created a new template-based stacking method (Fig. 2b), adapted the probability theory to incorporate geodetic data (eq. 1 and 2), and produced new scaling regressions (Fig. 3) to calculate fault displacement hazard maps (Fig. 4). This work has resulted in one publication so far (Milliner & Donnellan, 2020), an oral and poster presentation at conferences and will culminate in another publication that will outline the methodology we developed and the regressions that underpin the geodetic-based PFDHA approach. We anticipate future work will handle the varying uncertainties between datasets and their covariances, which will be addressed by using a mixed effects modeling approach. Another important outcome is that this project has allowed us to establish new collaborations across disciplines from engineers at UCLA to hazard practitioners in state, federal and private entities, which we expect will help strengthen the PFDHA community to push forward and tackle new problems. Lastly, this study has led us to securing a large scale 3-year NASA ROSES-ESI project to fully expand the geodetic-based PFDHA method, which will also help support a new version of COSI-Corr to measure the full 3D surface displacement field (which currently resolves only the horizontal motion).

E. References

Chen, R., Petersen, M.D., 2011. Probabilistic Fault Displacement Hazards for the Southern San Andreas Fault Using Scenarios and Empirical Slips. Earthq. Spectra 27, 293–313. https://doi.org/10.1193/1.3574226

Dunham, E.M., Belanger, D., Cong, L., Kozdon, J.E., 2011. Earthquake Ruptures with Strongly Rate-Weakening Friction and Off-Fault Plasticity, Part 1: Planar FaultsEarthquake Ruptures with Strongly Rate-Weakening Friction and Off-Fault Plasticity, Part 1: Planar Faults. Bull. Seismol. Soc. Am. 101, 2296–2307. https://doi.org/10.1785/0120100075

Graves, R., Jordan, T.H., Callaghan, S., Deelman, E., Field, E., Juve, G., Kesselman, C., Maechling, P., Mehta, G., Milner, K., Okaya, D., Small, P., Vahi, K., 2011. CyberShake: A Physics-Based Seismic Hazard Model for Southern California. Pure Appl. Geophys. 168, 367–381. https://doi.org/10.1007/s00024-010-0161-6

Ma, S., Andrews, D.J., 2010. Inelastic off-fault response and three-dimensional dynamics of earthquake rupture on a strike-slip fault. J. Geophys. Res. Solid Earth 115. https://doi.org/10.1029/2009JB006382

Manighetti, I., Campillo, M., Sammis, C., Mai, P.M., King, G., 2005. Evidence for self-similar, triangular slip distributions on earthquakes: Implications for earthquake and fault mechanics. J. Geophys. Res. Solid Earth 110. https://doi.org/10.1029/2004JB003174

Milliner, C., Donnellan, A., n.d. Using Daily Observations from Planet Labs Satellite Imagery to Separate the Surface Deformation between the 4 July Mw 6.4 Foreshock and 5 July Mw 7.1 Mainshock during the 2019 Ridgecrest Earthquake Sequence. Seismol. Res. Lett. https://doi.org/10.1785/0220190271

Petersen, M.D., Dawson, T.E., Chen, R., Cao, T., Wills, C.J., Schwartz, D.P., Frankel, A.D., 2011. Fault Displacement Hazard for Strike-Slip FaultsFault Displacement Hazard for Strike-Slip Faults. Bull. Seismol. Soc. Am. 101, 805–825. https://doi.org/10.1785/0120100035

Rockwell, T.K., Lindvall, S., Dawson, T., Langridge, R., Lettis, W., Klinger, Y., 2002. Lateral Offsets on Surveyed Cultural Features Resulting from the 1999 İzmit and Düzce Earthquakes, Turkey. Bull. Seismol. Soc. Am. 92, 79–94. https://doi.org/10.1785/0120000809

Roten, D., Olsen, K.B., Day, S.M., 2017. Off-fault deformations and shallow slip deficit from dynamic rupture simulations with fault zone plasticity. Geophys. Res. Lett. 44, 7733–7742. https://doi.org/10.1002/2017GL074323

Scharer, K.M., Salisbury, J.B., Arrowsmith, J.R., Rockwell, T.K., 2014. Southern San Andreas Fault Evaluation Field Activity: Approaches to Measuring Small Geomorphic Offsets—Challenges and Recommendations for Active Fault Studies. Seismol. Res. Lett. 85, 68–76. https://doi.org/10.1785/0220130108

Youngs, R.R., Arabasz, W.J., Anderson, R.E., Ramelli, A.R., Ake, J.P., Slemmons, D.B., McCalpin, J.P., Doser, D.I., Fridrich, C.J., Swan, F.H., Rogers, A.M., Yount, J.C., Anderson, L.W., Smith, K.D., Bruhn, R.L., Knuepfer, P.L.K., Smith, R.B., dePolo, C.M., O'Leary, D.W., Coppersmith, K.J., Pezzopane, S.K., Schwartz, D.P., Whitney, J.W., Olig, S.S., Toro, G.R., 2003. A Methodology for Probabilistic Fault Displacement Hazard Analysis (PFDHA). Earthq. Spectra 19, 191–219. https://doi.org/10.1193/1.1542891

F.Figures

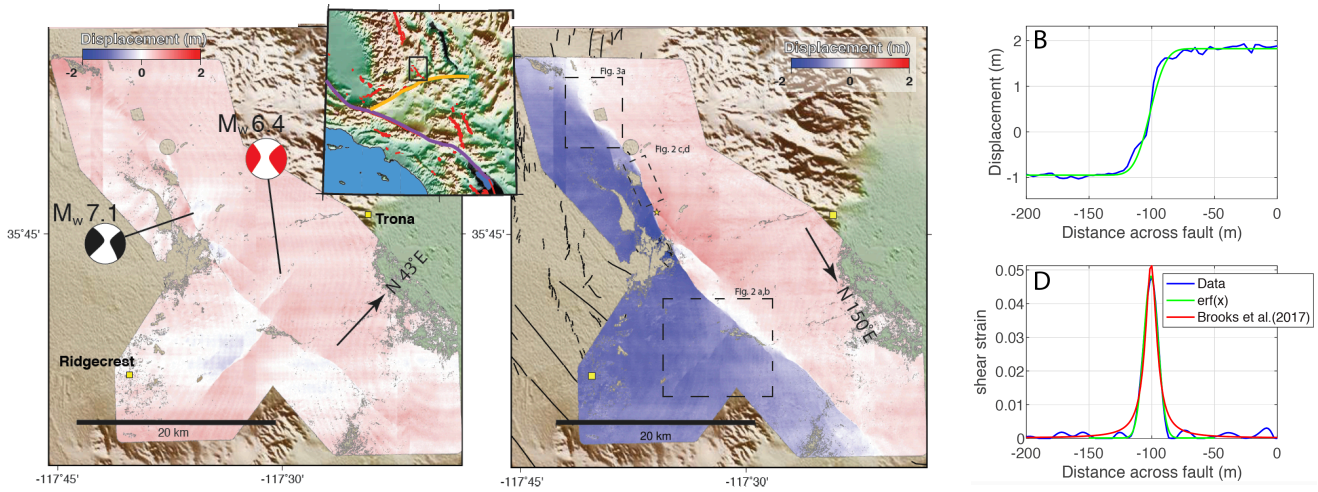

Fig. 1. Left two figures show the displacement map of the 2019 M_w 7.1 Ridgecrest earthquake from correlating SPOT-5 1.5 m resolution images, with displacement projected into the NE direction parallel to the Mw 6.4 faults (leftmost figure), and projected into the SE direction parallel to the strike of the mainshock faults (center figure). Right top shows a fault-parallel displacement profile and bottom right a fault-parallel shear strain profile estimated via central difference of top.

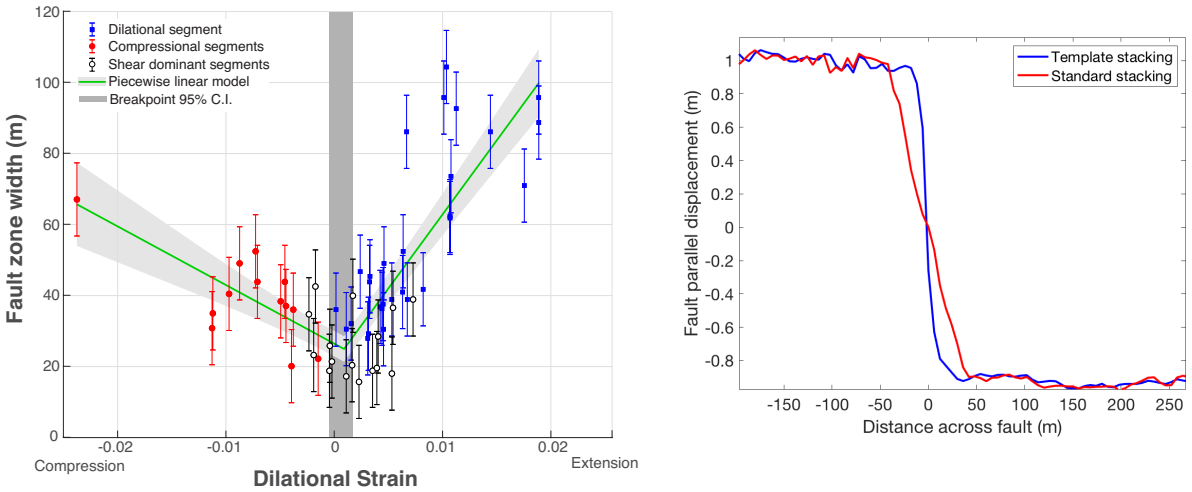

Fig. 2. Left, scaling regression showing the dependence of the fault zone width on the amount of dilation or compression a fault zone experiences. Right, illustration of the benefit of using our template-based stacking algorithm (blue) compared to standard stacking approach (red) which smooths the distribution of total displacement across the 2019 Ridgecrest surface rupture, widening the fault zone and lower the shear strain (gradient).

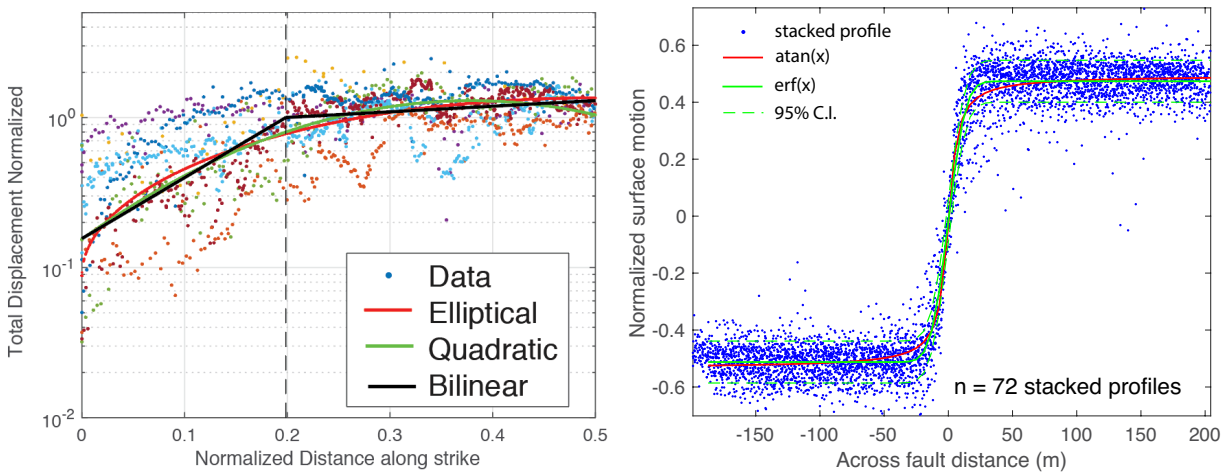

Fig. 3. Left, along fault displacement regression from 9 different earthquakes where different models have been fit including an elliptical, quadratic and bilinear. We find similar to Petersen et al. (2011) that a bilinear provides the best fit. Right, preliminary result of a FDPE constrained from displacement profiles measured along a segment of the 1992 Landers rupture. An error function (green line) is found to be better describe the variation of total displacement across the rupture than an artcan function (red line) which has a different curvature at the edges of the fault zone.

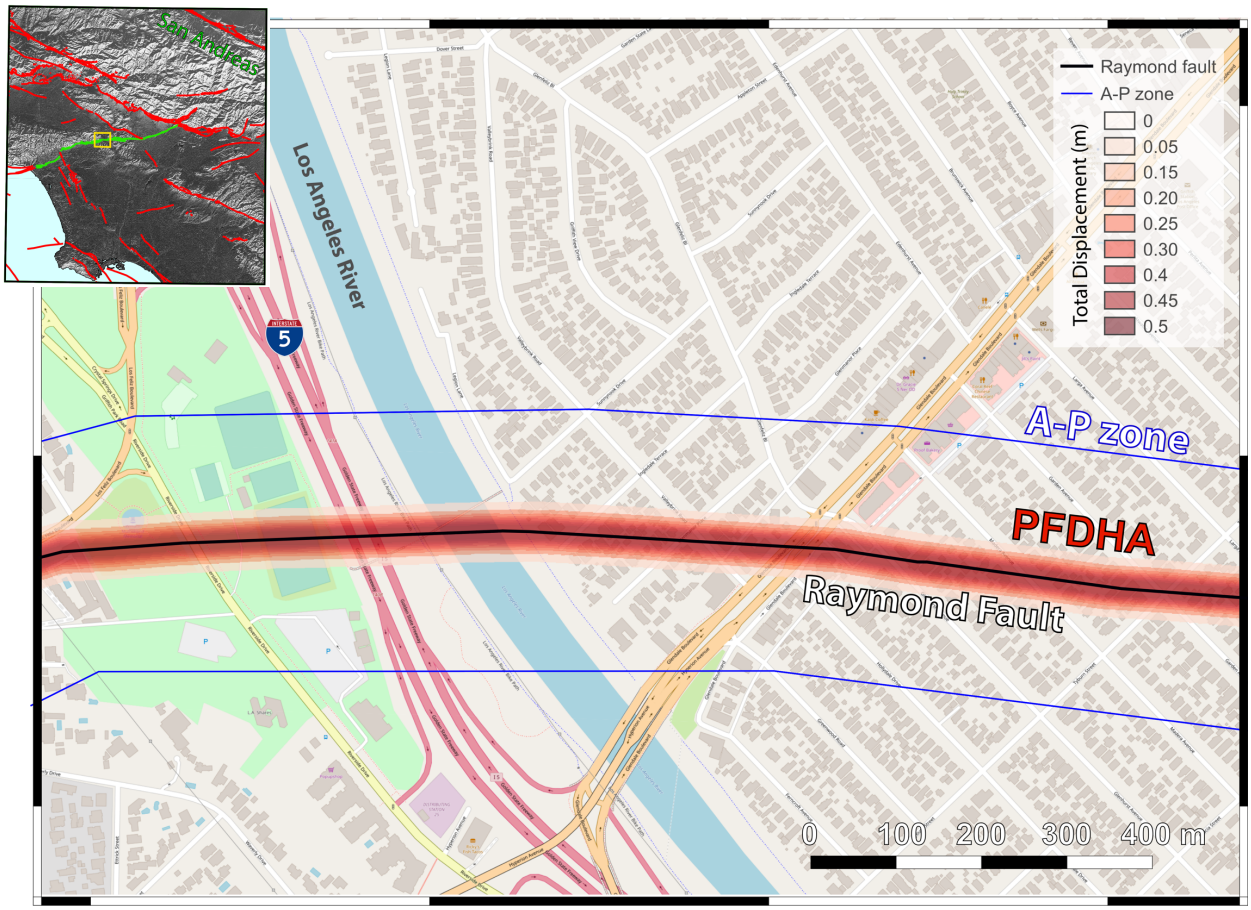

Fig. 4. Preliminary fault displacement hazard map produced from our geodetic-based PFDHA (eq. 1) shown as red areas along the Raymond fault in Los Angeles.